

The conversion of nata de coco bacterial cellulose into cellulose nanofibers using high shear mixer with eco-friendly fluid dynamics method

Amun Amri^{1*}, Diana Eka Putri¹, Dhina Febryza¹, Salsabilla Diva Voadi¹, Syelvia Putri Utami¹, Hussein A. Miran² and M. Mahbubur Rahman³


¹ Department of Chemical Engineering, Faculty of Engineering, Universitas Riau, **Indonesia**

² Department of Physics, College of Education for Pure Science, Ibn Al-Haitham, University of Baghdad, **Iraq**

³ Department of Physics, Jahangirnagar University, **Bangladesh**

* Corresponding Author: amun.amri@eng.unri.ac.id

Received October 26th 2024; Revised December 21st 2024; Accepted December 25th 2024

 Cite this <https://doi.org/10.24036/teknomekanik.v7i2.32972>

Abstract: Nanocellulose is widely applied in various fields due to its superior characteristics. Several methods have been developed to synthesize it, but they still have limitedness as being non-eco-friendly and inefficient use. Therefore, the synthesis of nanocellulose from sustainable sources is being developed using a simple and eco-friendly method. This study successfully produced a low viscosity gel suspension of cellulose nanofibers (CNF) from bacterial cellulose (BC) derived from Nata de Coco using a high shear mixer (HSM). The mixture of BC and water in a 1:1 ratio was processed with various rotational speeds and times in the HSM. The suspension result was characterized using an Ostwald viscometer, UV-vis spectrophotometer, lux meter, scanning electron microscopy (SEM), Fourier transform infrared spectroscopy (FTIR), particle size analyzer (PSA), and x-ray diffraction (XRD). Based on the characterization, it was confirmed that higher rotational speeds and extended processing times reduced the suspension viscosity and increased light transmittance, indicating a reduction in BC size to the submicron/nanometer scale. The best light transmittance was achieved with the HSM at 4500 rpm for 180 min, resulting in a viscosity drop from 232.67 mPa.s to 1.45 mPa.s. Scanning electron microscopy (SEM) and X-ray diffraction (XRD) analysis showed that the CNF retained its fibrous structure with nanometer-scale widths and high porosity without significant changes in crystallinity.

Keywords: high shear mixer; bacterial cellulose; cellulose nanofibers; viscosity; light transmittance

1. Introduction

Nanocellulose has attracted significant attention in materials research due to its superior properties, such as excellent mechanical strength, biocompatible, biodegradable, and high surface area [1], [2], [3]. Nanocellulose holds great promise for applications in biomedicine, energy storage devices, cosmetics, tissue engineering, 38 thickeners, nanocomposites, and more [4], [5], [6]. Bacterial cellulose (BC) is one of the potential raw materials for synthesizing nanocellulose. One of the BCs is Nata de Coco, a fermentation product of coconut water. Nata de coco is a potential material for making nanocellulose because the raw material (coconut water) is easy to find. In 2019, the global coconut plantation area was approximately 11.63 million hectares, in which the 79.1% was in Asia. Indonesia accounted for about 29.3% of the total coconut plantation area in Asia. The Directorate General of Estate Crops (DGEC) reported that Indonesia had 3.4 million hectares of coconut plantations, comprising 3.27 million hectares of tall coconut plantations, and the rest were hybrid coconut plantations [7].

The development of bacterial celluloses (BC) into nanocelluloses, such as cellulose nanofibers (CNF) and cellulose nanocrystals (CNC), offers enhanced material properties, making it lighter, more stable, stronger, and functional [8]. CNF has a long, flexible fiber network, and a larger diameter than CNC, making it suitable for various applications [3]. CNF from BC can be synthesized through various methods, including chemical, biological, and mechanical approaches. Chemical methods typically involve hydrolysis using strong acids such as sulfuric, bromic, and hydrochloric acids. However, this method has disadvantages, such as health and environmental risks, low yield, and significant cellulose degradation [9], [10]. However, more eco-friendly biological methods face challenges in isolating pure enzymes and require long processing times. On the other hand, mechanical methods utilize equipment to reduce the BC particle size to produce CNF. This process offers a safer and more eco-friendly alternative [11].

Nano-sized particles of bacterial cellulose have been successfully synthesized using a mechanical method with a blender, followed by acid hydrolysis with sulfuric acid and then grinding [12]. XRD analysis showed that the crystal size obtained was approximately 9.11 nm, with a crystallinity index of approximately 67.27%. However, the particle size remained relatively large, approximately ~30-60 μm , showing inhomogeneous [12]. Nanocellulose can be synthesized from BC [13] using the aqueous counter collision (ACC) method, where cellulose fibers are broken down to the nanoscale using a colliding water flow. The resulted nanocellulose fibers measured about ~30 nm and retained over 70% crystallinity. However, these fibers tended to aggregate, and beyond a certain point, further size reduction could not be achieved [13]. Nano-sized particles of BC were synthesized [10] through ultrasonic process, resulting in transparent nanofiber suspension with porous structure and diameter of 60 nm. The sonication process used sound energy to create acoustic cavitation, causing the cutting and reduction of cellulose particle size. However, this method requires high costs and power consumption [10].

Previous methods have several disadvantages, such as the combination of mechanical and chemical methods makes the process less eco-friendly. There is also agglomeration of nanocellulose beyond a certain threshold. This study examines the use of high shear mixer to synthesize SNF from bacterial cellulose (BC). It is easier and more efficient because it does not have many steps in the process and does not cause pollution. The use of high shear mixer is very efficient in processing large volumes, with energy efficiency reaching for 70% to 80%, thus allowing reduced energy consumption [14]. Furthermore, the HSM method relies only on mechanical principles without any combination with chemical methods. The working mechanism of the HSM is based on hydrodynamic forces, including shear forces, particle collisions, and jet cavitation, which lead to the breakdown and reduction of BC particles to the nanoscale [15], [16]. This work utilized HSM to convert BC of Nata de Coco to CNF using HSM in various rotational speed (rpm) and processing time. HSM can significantly reduce costs and energy consumption compared to ultrasonic mechanical methods. In this process, the CNF produced from BC exhibits a web-like structure's high porosity, and homogeneous particle size, making it a promising, straightforward, and eco-friendly approach for synthesizing high-quality CNF.

2. Material and methods

2.1 Synthesis of Cellulose Nanofiber (CNF)

Bacterial cellulose (BC) was produced through the fermentation of coconut water by using *Acetobacter Xylinum*. The process began by boiling 5 liters of coconut water. Once it boils, 500 grams of white sugar, 25 grams of ammonium sulfate, and 30 mL of glacial acetic acid were added. About 300 mL of the prepared solution was poured into a plastic container, sealed, and cooled to room temperature. The addition of glucose served as a culture medium and a carbon source, while ammonium sulfate functioned as a nitrogen source in the bacterial metabolism process. Glacial

acetic acid was added to create an acidic environment to support optimal bacterial growth. *Acetobacter xylinum* is required to optimize bacterial cellulose production. After cooling, *Acetobacter xylinum* was added at 10% of the medium's volume, and the mixture was fermented for 7 days. Once fermentation was completed, the resulted bacterial cellulose was soaked and washed with hot water to remove residual impurities and improve its quality [17]. The obtained BC was cut into smaller pieces and then mixed with water at a BC-to-water weight ratio of 1:1. CNF was synthesized from the BC and water mixture through mechanical treatment using three different fluid dynamics routes. The first route involved fluid dynamics processing using a kitchen blender at a speed of 15000 rpm for 5 minutes. The second route combined fluid dynamics with a kitchen blender for 5 minutes, followed by ultrasonication at 50°C with various ultrasonic durations (30, 60, and 90 minutes). The third route combined fluid dynamics using a kitchen blender for 5 minutes, followed by further processing with an HSM at different rotational speeds (1500, 3000, and 4500 rpm) and various durations (60, 120, and 180 minutes).

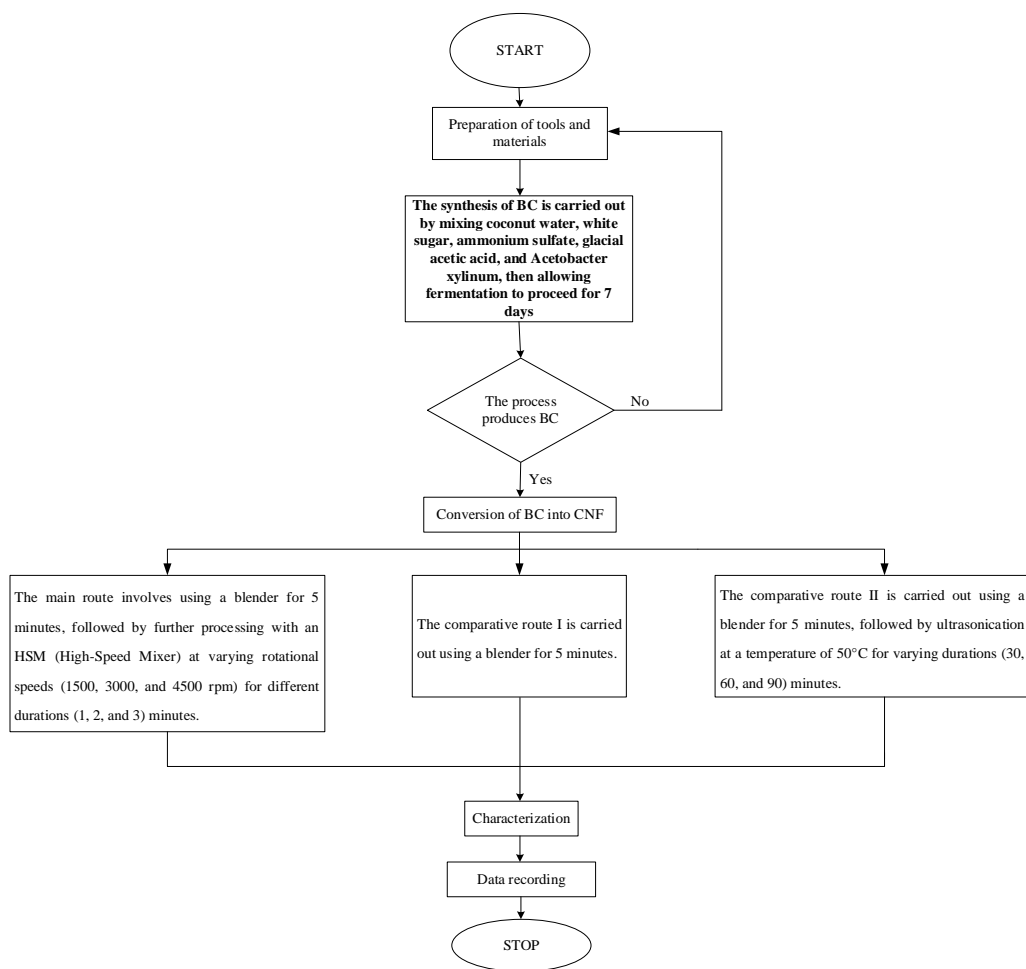


Figure 1. Flow diagram of Cellulose Nanofiber Synthesis Fluid Dynamic in High Shear Mixer with various different routes

2.2 Characterization

The light intensity of the sample was measured using a digital lux meter AS803. Visual observations to evaluate the total percentage of light transmitted through the sample were conducted using a UV-vis spectrophotometer at a wavelength of 400 nm [18]. The sample's viscosity was measured using an Ostwald viscometer [19]. Based on the results of visual characterization of light transmittance, light intensity, and viscosity, three samples were selected: the worst result, the best result, and the initial sample. Functional group analysis was performed using a PerkinElmer

Spectrum IR Version 10.6.1 instrument. Crystallinity index analysis was conducted using a PanAnalytical instrument with a 2θ angle, and CuK α radiation at 1.54060 nm. CuK α radiation and operating with a step size of 0.01° . Further analysis of the 2D peaks was performed using OriginPro software. Further analysis was conducted to calculate the crystallinity index (CI) using the Segal method, formulated in Equation 1.

$$CI (\%) = \frac{I_{002} - I_{am}}{I_{002}} \times 100 \quad (1)$$

Where I_{002} is the maximum intensity of the diffraction peak from the (002) plane at a 2θ angle around 22° and 23° , and I_{am} is the minimum intensity of the amorphous phase diffraction taken at a 2θ angle between 15° - 19° [10], [12]. The average crystallite size is calculated using the Debye-Scherrer equation at the diffraction peak of the (002) lattice plane, as shown in Equation 2 [12], [20].

$$D (nm) = \frac{K\lambda}{\beta \cos \theta} \quad (2)$$

Where K is the Scherrer constant (0.9), λ is the wavelength of the light used (Cu, $\lambda = 0.15406$ nm), β is the full width at half maximum (FWHM) (in radians), and θ is the diffraction angle (in radians) [20], [21]. Morphological analysis was carried out by using a SEM FEI Inspect-S50 instrument with a voltage of 20 kV. PSA testing was conducted on a Horiba Scientific SZ-100 instrument applying the scattering light intensity method, with further analysis performed using OriginPro software.

3. Results and discussion

3.1 Visual observation of light transmittance

Figure 2 shows the suspension obtained from processing Nata de Coco using a blender for 5 minutes, ultrasonication, and a high-shear mixer (HSM) with mixer speed and processing time variations. The HSM sample (4500 rpm, 180 minutes) visually appeared more transparent than the other samples. This result indicates that nano-sized fiber suspensions tend to be more transparent than micro-sized fibers [10]. This means that smaller particle size will lead to an increase in transparency. Transparency and suspension homogeneity significantly increase with longer processing times [10].

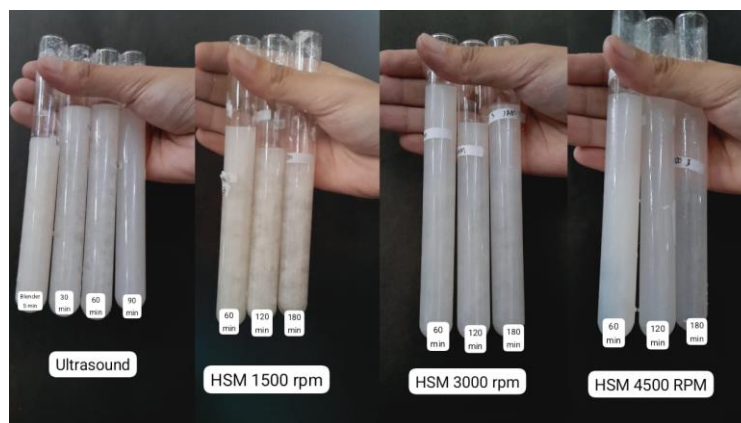


Figure 2. Visual appearance of the conversion results of Nata de coco into nanocellulose at various mixer speeds (rpm) and processing times (t)

Figure 3 shows the quantitative test results for light intensity passing through the liquid suspension, measured using a lux meter. As seen in Figure 3, the highest light intensity was obtained for the HSM sample (4500 rpm, 180 minutes). Longer processing times and higher mixing speeds can enhance the fragmentation of cellulose fibers into smaller, finer particles [22]. Smaller and finer particles have better capabilities for scattering and transmitting light, which enhances light intensity [23]. The working mechanism of HSM is based on hydrodynamic forces, including shear forces, jet cavitation, and collisions, which accelerate the fragmentation of cellulose fibers into a more homogeneous nanoscale [16], [24]. Smaller, finer nanocellulose particles allow more light to be transmitted or reflected, reducing light resistance and increasing the light intensity measured by the lux meter. Smaller particle sizes improve optical transparency and enhance light transmittance [25].

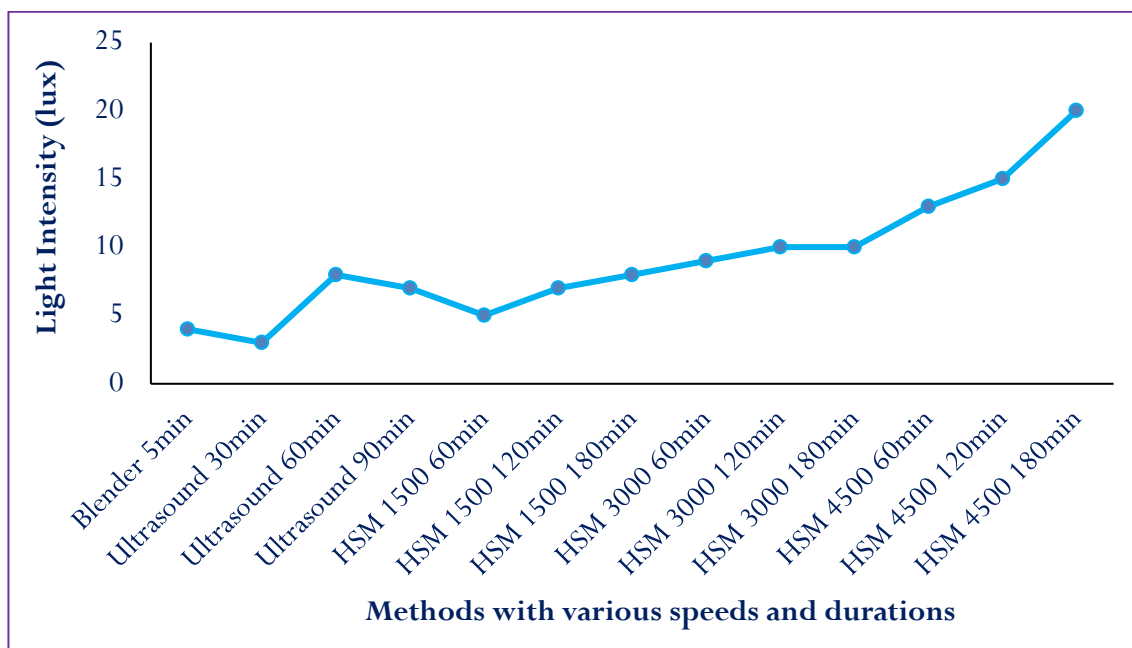


Figure 3. Light intensity test results using a lux meter

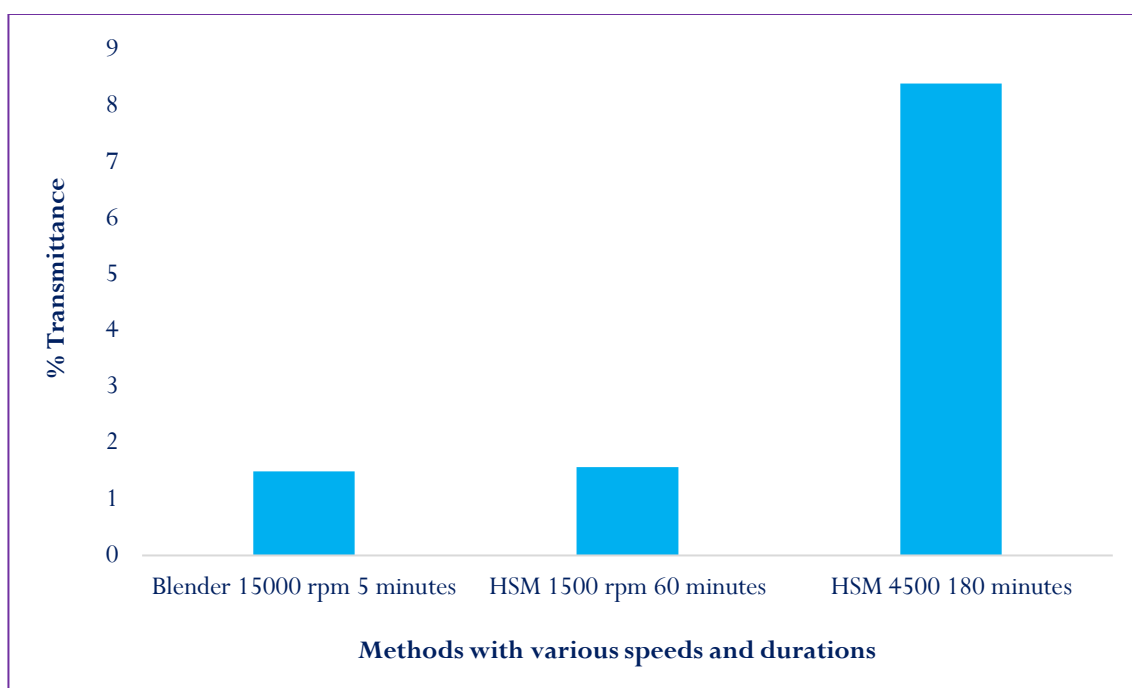


Figure 4. Light transmittance measurement using a UV-VIS spectrophotometer

Figure 4 illustrates the measurement results using a UV-Vis spectrophotometer at a wavelength of 402 nm. Absorbance is inversely proportional to transmittance. Absorbance is the amount of light absorbed, while transmittance is the amount of light transmitted [26]. Figure 4 shows that the suspension obtained at a mixing speed of 4500 rpm and a processing time of 180 minutes has a light transmittance value for 5.6 times greater than the initial Nata de Coco (blender 15000 rpm for 5 minutes). Fewer molecules absorb light, allowing more light to pass through the sample. Higher crystallinity tends to increase back reflection and reduce absorbance due to increased light scattering, increasing light transmittance [27], [28]. Therefore, higher mixing speeds and longer processing times lead to decreased absorbance and increased transmittance.

3.2 Viscosity analysis

Figure 5 shows the viscosity measurement results for each sample using an Ostwald viscometer. Nanocellulose has a higher viscosity than water due to strong hydrogen bonds between its fibers, which allows for a stable network in solution and increases viscosity [29]. Higher mixing speeds and longer mixing times (HSM, 4500 rpm, 180 minutes) decrease the viscosity of nanocellulose; this is because the cellulose fibers in suspension are cut into smaller sizes, reducing the molecular chain length and its ability to form a cohesive network [30]. The highest viscosity (232.66 mPa.s) and lowest viscosity (1.45 mPa.s) were observed in the samples processed with a blender for 5 minutes and with HSM (4500 rpm, 180 minutes), respectively, showing a 160-fold reduction in viscosity; this demonstrates that the HSM process effectively breaks the fiber bonds in Nata de Coco. The high viscosity values are due to particle structure, cohesive forces [31], and hydrogen/Van der Waals bonds, which are disrupted by the shear forces in the HSM.

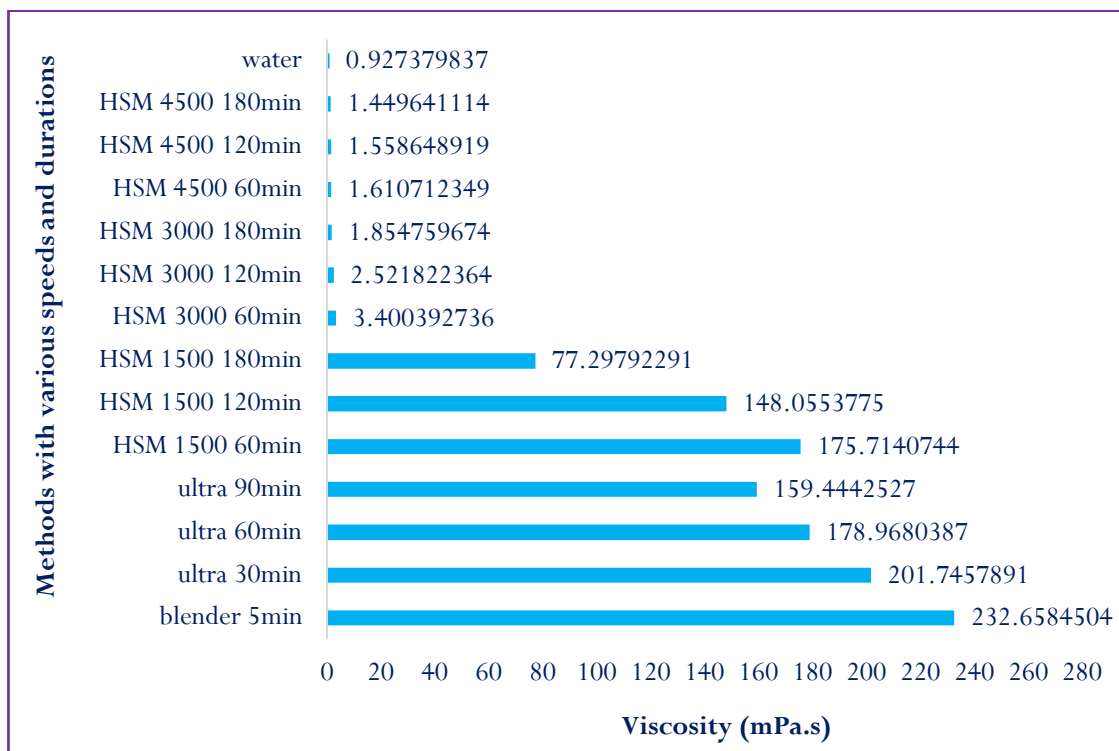


Figure 5. Viscosity values of samples (mPa.s)

3.3 Structural of morphology analysis

Figure 6 presents the SEM characterization results for samples (a) blender for 5 minutes, (b) HSM (1500 rpm, 60 minutes), and (c) HSM (4500 rpm, 180 minutes). Overall, it can be observed that nanocellulose exhibits long, interconnected fiber strands originating from the solid nata de coco,

which has been cut down through mechanical treatment [32]. In Figure 6 (a), the structure appears less homogeneous, with relatively larger pores. This indicates that the mechanical process of blender 5 min was not optimal, leaving the fibers with a coarser texture at a micro-scale. Figure 6 (b) shows that most fibers have been reduced to the nanometer scale, with diameters of approximately 78.49 nm and 169.40 nm, finer pore networks, and a more organized structure. Figure 6 (c) displays a web-like nanostructure with diameters of approximately 55.98 nm and 84.51 nm, a higher distribution of pores, and more homogeneous fibers. This finding is consistent with previously reported findings that mechanical treatment can produce cellulose fibers with diameters below 100 nm [33], [34]. Aggregated web-like structures consisting of interwoven nano-threads, known as nanofibrils, in bacterial cellulose sheets derived from nata de coco [32]. Additionally, Figure 6 (c) shows that the sample has higher porosity, as the nanofiber structure forms multiple fiber networks, creating more empty spaces between fibers. High porosity in nanocellulose is crucial in various applications, including tissue engineering, gas sensors, fuel cells, catalysis, fluid purification and filtration, and protein immobilization and separation [32].

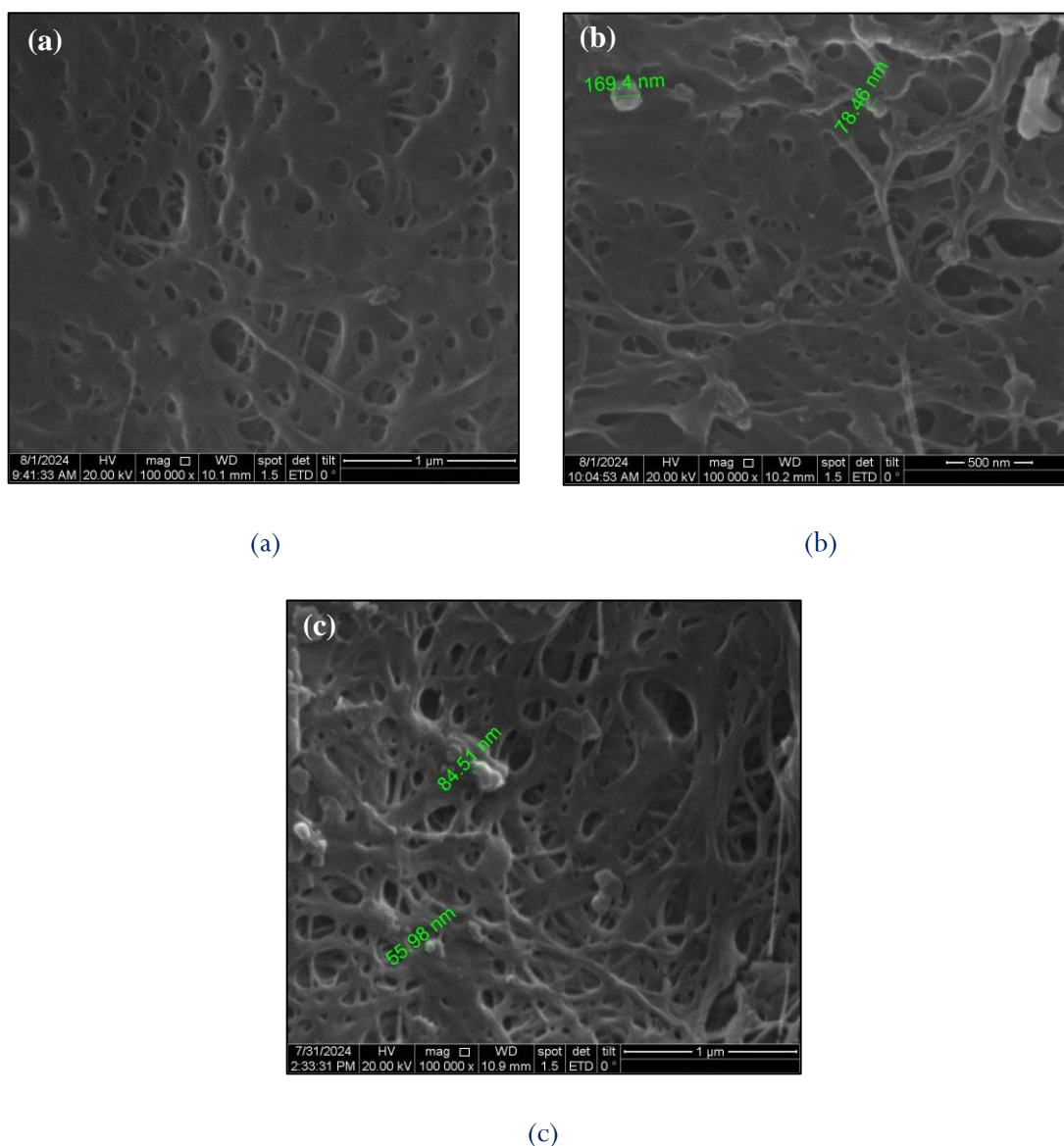


Figure 6. SEM analysis: (a) Blender 5 min, (b) HSM (1500 rpm, 60 min), and (c) HSM (4500 rpm, 180 min)

Figure 7 presents the SEM-EDX patterns for (a) blender 5 minutes, (b) HSM (1500 rpm, 60 minutes), and (c) HSM (4500 rp, 180 minutes). Elemental analysis of nanocellulose was conducted

using energy-dispersive X-ray spectroscopy (EDX). Figure 7 presents the percentage of elements found in the nanocellulose samples. All treatments indicated similar elemental compositions, with the dominant elements being C and O. Carbon (C) is the primary element in nanocellulose. At the same time, oxygen (O) is crucial as it forms part of the hydroxyl group (-OH) in the nanocellulose structure [35]. Figure 7 illustrates that, across the three samples, the weight percentage of C ranged from 58.4% to 64.4%, with the highest percentage observed in the high shear mixer treatment for 180 minutes, while the weight percentage of O ranged from 33.8% to 40.6%. The results support the study on characterized nanocellulose elements using EDX, finding 71.04% for C, 24.85% for O, and very low percentages for other elements, such as Mg, S, Na, Cl, K, and Ca [36]. Sodium (Na) and magnesium (Mg) originated from the bacterial cellulose fermentation process were used as a fermentation medium, while the other trace elements were likely resulted from processing or contact with equipment during sample preparation [37].

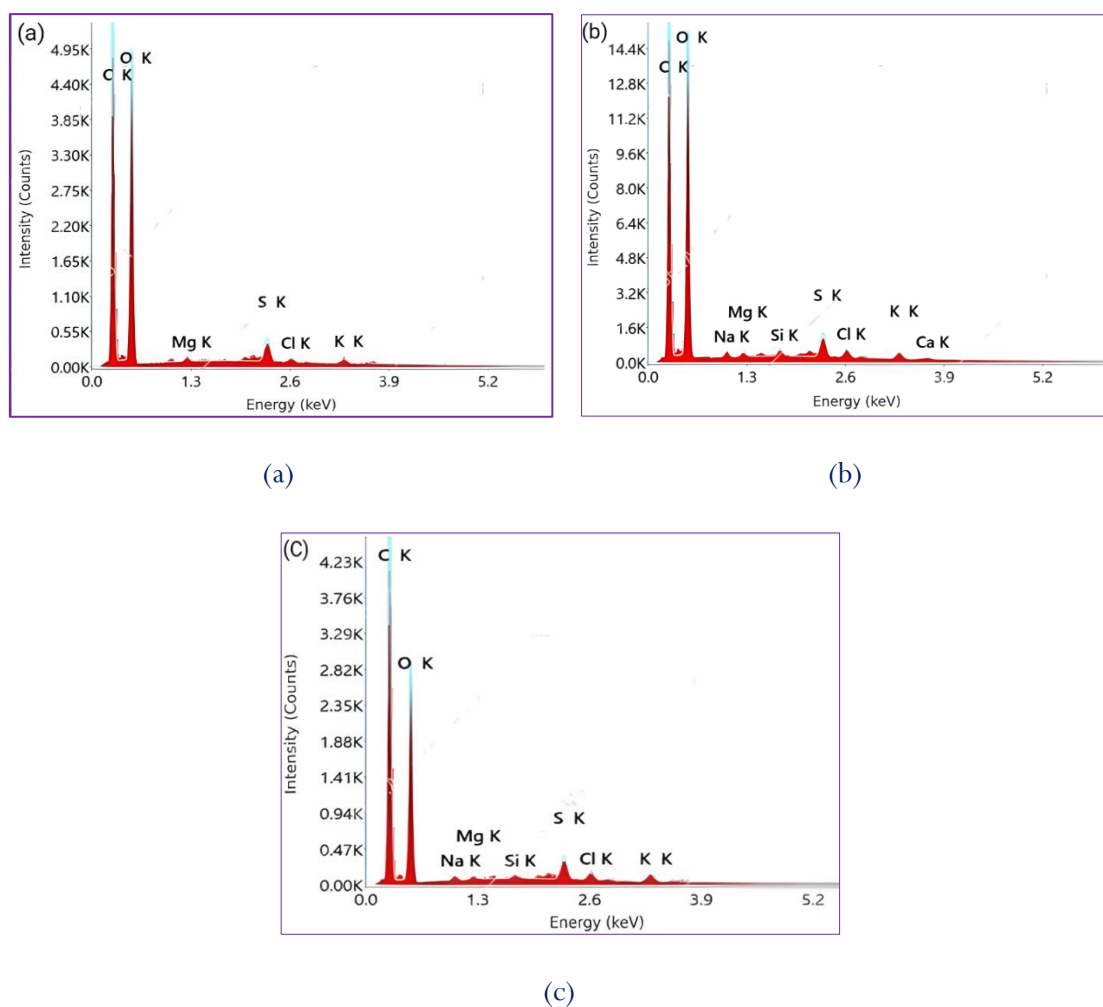


Figure 7. SEM-EDX analysis: (a) blender 5 min, (b) hsm (1500 rpm, 60 min), and (c) hsm (4500 rpm, 180 min)

Table 1. Elemental weight percentage

Variable	%Weight								
	C	O	Mg	S	Cl	K	Na	Si	Ca
Blender 5 min	58.4	40.6	0.1	0.6	0.1	0.2	0	0	0
HSM 60 min	58.5	39.9	0.1	0.6	0.2	0.2	0.2	0.1	0.1
HSM 180 min	64.6	33.8	0.1	0.7	0.2	0.3	0	0.1	0

3.4 Functional group analysis

Figure 8 presents the FTIR test results for samples processed with a blender for 5 minutes (red), HSM (1500 rpm, 60 minutes) (black), and HSM (4500 rpm, 180 minutes) (blue). Generally, each sample shows a broad peak at approximately $\sim 3337.60 \text{ cm}^{-1}$ - 3339.30 cm^{-1} due to the stretching vibration of hydroxyl groups (O-H), indicating the presence of water molecules in the sample [12], [32], [38]. The HSM sample (4500 rpm, 180 minutes) shows a broad O-H peak with reduced intensity, suggesting more orderly hydrogen interactions [39]. Higher mixing speeds and longer processing times result in decreased intensity and a shift in the O-H peak, indicating the breaking of chains in bacterial cellulose [10], [40]. Additionally, each sample shows a small peak at approximately $\sim 2100 \text{ cm}^{-1}$ associated with $\text{C}\equiv\text{C}$ bond stretching [10], [41]. The high-intensity but narrow peak at approximately $\sim 1637 \text{ cm}^{-1}$ in each sample is due to the stretching of $\text{C}=\text{C}$ bonds from the alkene functional group [32], [41]. The HSM samples show peaks at approximately $\sim 1320 \text{ cm}^{-1}$ and 1431 cm^{-1} , associated with C-H bending and CH_2 bending from the alkane (cellulose) functional group [41].

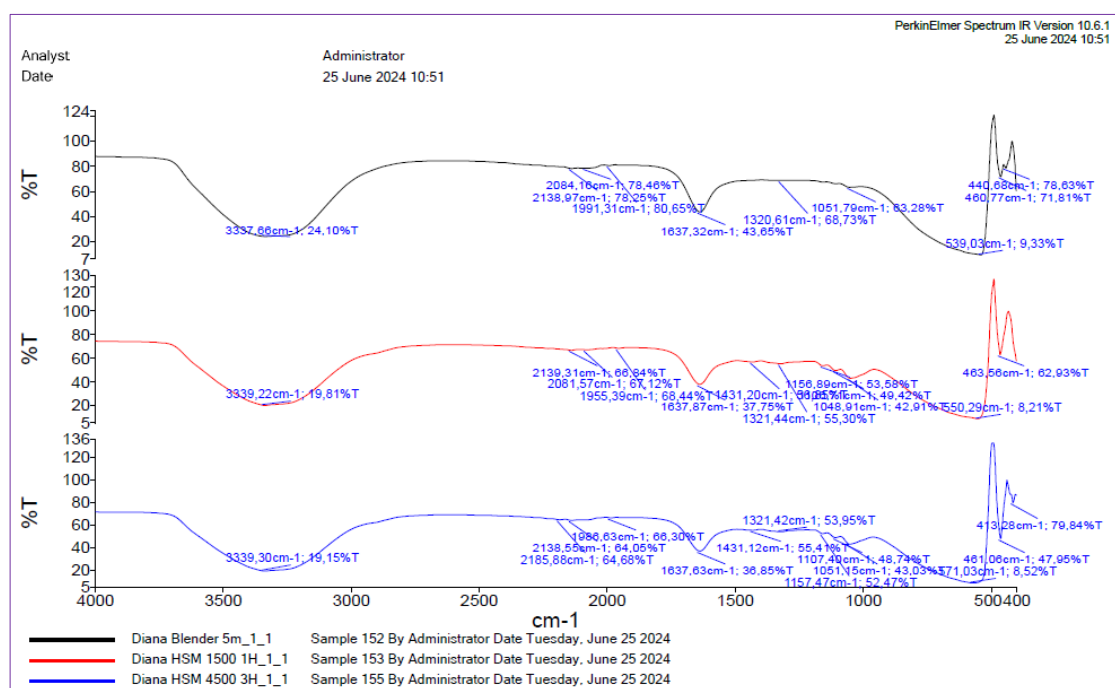


Figure 8. FTIR analysis results

In Figure 8, other significant peaks can be observed at approximately ~ 1160 - 1100 cm^{-1} and $\sim 1050 \text{ cm}^{-1}$, associated with the asymmetric stretching vibrations of the O-C-O and C-O bonds from the alcohol functional group (cellulose) [12], [38], [41]. Peaks at approximately $\sim 1429 \text{ cm}^{-1}$, 1163 cm^{-1} , and 1111 cm^{-1} indicate cellulose type I β [42]. Peaks between 850 - 400 cm^{-1} represent a region with bands corresponding to heavy-atom bending and rotation [43]. Peaks at approximately ~ 89 - 898 cm^{-1} are caused by the glycosidic linkage between glucose units in cellulose [44].

3.5 Particle Size Analyzer (PSA)

Figure 9 shows the PSA curve patterns for the samples processed with (a) a blender 15000 rpm for 5 minutes, (b) HSM at 1500 rpm for 60 minutes, and (c) HSM at 4500 rpm for 10 minutes. The Y-axis represents intensity distribution (percentage), and the X-axis represents particle size. The blue bar chart shows intensity distribution by particle size. At the same time, the red line indicates the undersize percentage of the sample, representing the cumulative proportion of particles smaller

than the specified size [45]. The average particle sizes of the samples processed with the blender for 5 minutes, HSM (1500 rpm, 60 minutes), and HSM (4500 rpm, 180 minutes) were approximately 1639.70 nm, 1173.10 nm, and 599.50 nm, respectively.

Figure 9, illustrates that significant cellulose particle size reduction occurs at higher rotational speeds and longer processing times. At lower speeds, shear forces are not strong enough to break particles into smaller sizes. Conversely, higher speeds and longer durations increase shear force and turbulence, leading to more effective cellulose particle fragmentation [46]. The visible smallest structural unit of cellulose I is a bundle of parallel glucan chains, commonly known as cellulose I fibrils [47]. These fibrils are held together by a network of hydrogen bonds and Van der Waals forces, aggregating into larger fibril aggregates [47]. High shear forces generated by the rapid rotation of the rotor against the stator in HSM (4500 rpm, 180 minutes) are able to reduce the initial fibril aggregate size from ~ 1639.70 nm to approximately ~ 599.50 nm. This mechanism can be explained by the breaking of hydrogen bonds and Van der Waals forces between fibers that form cellulose fibril aggregates under high shear force, leading to nanocellulose particle size reduction without damaging the crystalline and amorphous structure [47].

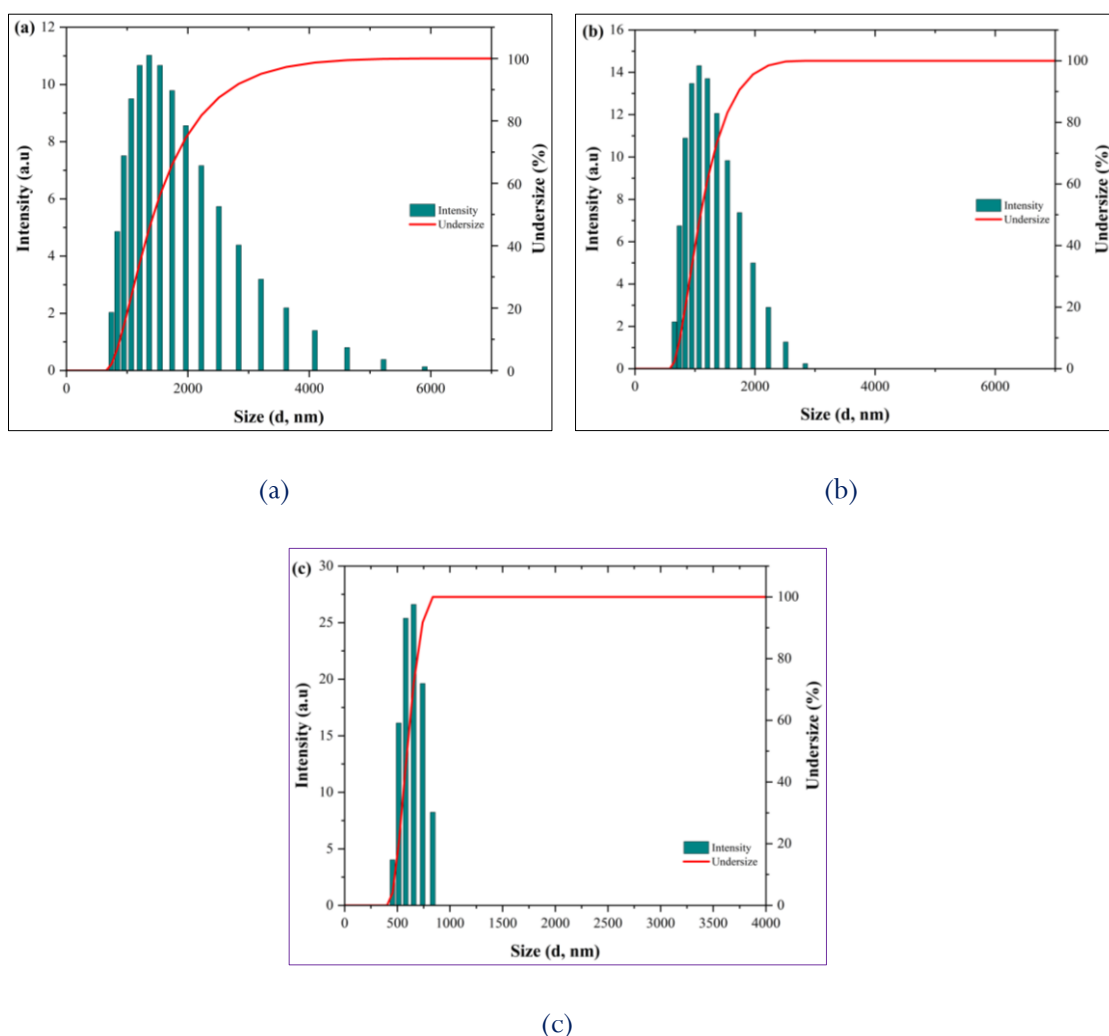


Figure 9. PSA test results from (a) blender for 5 minutes; (b) HSM at 1500 rpm for 60 minutes; and (c) HSM at 4500 rpm for 180 minutes

Figure 9 (a) shows a wider particle size distribution with a lower peak, indicating many particles with various sizes. In contrast, Figure 9 (b) shows a narrower particle size distribution within a smaller size range (< 3000 nm), indicating improved homogeneity. Figure 9 (c) displays the

narrowest particle size distribution, with a more concentrated size range (< 1000 nm) and a higher peak, signifying highly homogeneous particle sizes [48], [49], [50]. Higher rotational speeds and longer processing times increase the homogeneity of nanocellulose particles. Narrow particle size distribution is crucial for the stability, consistency, and performance of nanomaterials in various applications. The functionality of nano-based devices improves with homogeneous nano-particle size distribution [48], [51].

3.6 Crystallinity index analysis

Figure 10 shows the XRD characterization results for samples processed with a blender (5 minutes), HSM (1500 rpm, 60 minutes), and HSM (4500 rpm, 180 minutes). The diffraction peaks in the diffractogram are due to crystal scattering, while the diffuse background is due to amorphous regions. According to the International Centre for Diffraction Data (ICDD), the diffraction peaks of native cellulose are located around $2\theta = 14.90^\circ$, 16.49° , and 22.84° , corresponding to the crystal planes (001), (110), and (002), respectively [12]. The XRD patterns of each sample show diffraction peaks at 2θ positions around 14.52° - 14.65° , 16.63° - 16.73° , and 22.73° - 22.84° , indicating the presence of crystalline cellulose type I structure [52]. These values align with ICDD data, showing the presence of the I β polymorph typically found in bacterial cellulose (BC) [12]. These three peaks serve as primary indicators confirming that each sample retains the crystalline structure of cellulose type I β , despite undergoing various mechanical treatments [12]. However, there is no change in the cellulose crystal structure during nanocellulose conversion.

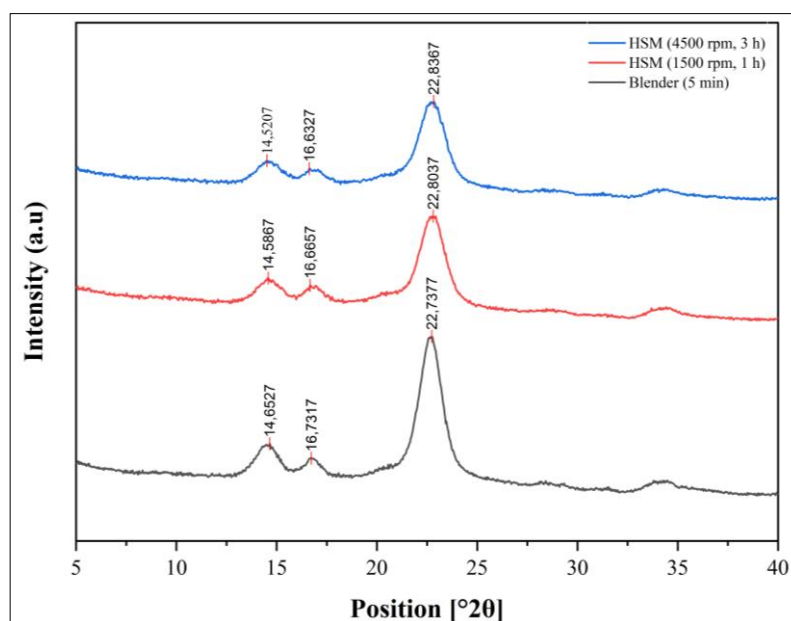


Figure 10. XRD diffraction pattern of different mixer speed and processing time of HSM

Table 2. shows the crystallinity index (X_{002}) values and crystallite size (D_{002}). In Figure 9, presents that mechanical treatment at higher speeds and longer durations tends to produce broader XRD peaks which correspond to smaller crystallite sizes [12]. These results are consistent with the average crystallite size calculations shown in Table 1. The friction and impact forces generated by the blender at 15000 rpm, HSM 1500 rpm and HSM 4500 cause the cellulose fibers to fragment into smaller crystallite sizes [53]. Bacterial cellulose has high structural resilience, especially in the crystalline regions, so crystallinity does not significantly change although having been through mechanical processing [53]. Structural resilience is able to enhance thermal stability because these bonds help prevent degradation or chain scission of polymers at high temperatures. Similar properties are found in CNF produced from plant cellulose which also possesses good thermal and

chemical stability, making it a potential candidate for applications in electrochemical sensor electrodes. However, since CNF is not conductive, modification with materials that have high conductivity is needed to improve electrode performance [54], [55]. The resulted crystallinity index shows that mechanical processing does not significantly affect the amorphous and crystalline structure of cellulose but rather reduces its size. The obtained crystallinity index aligns with the finding of previous study, showing a crystallinity index of ~59.50% for bacterial cellulose underwent a mechanical processing [32].

Table 2. Crystallinity index (X_{002}) and crystallite size (D_{002}) Values

Sample	D_{002} Nm	X_{002} %
Blender 5 min	6.09	59.20
HSM (1500 rpm, 60 min)	5.06	58.30
HSM (4500 rpm, 180 min)	3.24	54.80

4. Conclusion

Cellulose Nanofiber (SNF) has been successfully synthesized using a mechanical high shear mixer method. The results of functional group characterization, light transmittance, viscosity, particle size distribution, crystallinity index, and morphology analysis support the findings. The study revealed that the sample processed at 4500 rpm for 180 minutes achieved the desired nanocellulose properties, with the smallest diameter measured at 55.98 nm. However, this research has not succeeded yet in breaking down and enhancing the crystalline structure of the nanocellulose. Future studies are suggested to utilize different raw materials for BC production and experiment with various rotation speed and processing time. However, this method potentially produces CNF in a practical way without requiring additional chemicals, leading it to be an eco-friendly method.

Author's declaration

Author contribution

Amun Amri: conceptualization, funding acquisition, methodology, resources, supervision. **Diana Eka Putri:** investigation, data curation, formal analysis, writing - Original Draft. **Dhina Fabryza:** modelling, software, review. **Salsabilla Diva Voadi:** investigation, data curation, formal analysis, writing - Original Draft. **Syylvia Putri Utami:** investigation, writing - Review & Editing. **Hussein A. Miran:** writing - Review & Editing. **M. Mahbubur Rahman:** validation, writing - Review & Editing.

Funding statement

This research was funded by the Directorate General of Higher Education, Research, and Technology, Republic of Indonesia.

Acknowledgements

We would like to express our sincere gratitude to the Directorate General of Higher Education (DIKTI), Ministry of Education, Culture, Research, and Technology of the Republic of Indonesia for the financial support provided through the research funding program. We would also like to extend our thanks to all individuals and institutions who have contributed for the completion of this study.

Competing interest

The authors declare that no known financial or personal interests that could be interpreted as influencing or compromising the integrity of the work presented in this paper.

Ethical clearance

This research does not involve humans as subjects.

AI statement

The grammatical structure of this article was corrected by Grammarly and the authors have re-checked the accuracy and suitability of the sentences produced with the topic and data of this research. The language use in this article has been validated and verified by an English language expert and found no AI-generated sentence is included in this article. However, the authors are fully responsible for all the content of this article.

Publisher's and Journal's note

Universitas Negeri Padang as the publisher, and the editor of Teknomekanik state that there is no conflict of interest towards this article publication.

References

- [1] B. Thomas *et al.*, "Nanocellulose, a Versatile Green Platform: From Biosources to Materials and Their Applications," *Chemical Reviews*, vol. 118, no. 24, pp. 11575–11625, Dec. 2018, <https://doi.org/10.1021/acs.chemrev.7b00627>
- [2] P. Phanthong, P. Reubroycharoen, X. Hao, G. Xu, A. Abudula, and G. Guan, "Nanocellulose: Extraction and application," *Carbon Resources Conversion*, vol. 1, no. 1, pp. 32–43, Apr. 2018, <https://doi.org/10.1016/j.crcon.2018.05.004>
- [3] T. W. Kurniawan, H. Sulistyarti, B. Rumhayati, and A. Sabarudin, "Cellulose Nanocrystals (CNCs) and Cellulose Nanofibers (CNFs) as Adsorbents of Heavy Metal Ions," *Journal of Chemistry*, vol. 2023, pp. 1–36, Mar. 2023, <https://doi.org/10.1155/2023/5037027>
- [4] W. Chen, H. Yu, S.-Y. Lee, T. Wei, J. Li, and Z. Fan, "Nanocellulose: a promising nanomaterial for advanced electrochemical energy storage," *Chemical Society Reviews*, vol. 47, no. 8, pp. 2837–2872, 2018, <https://doi.org/10.1039/C7CS00790F>
- [5] D. Klemm *et al.*, "Nanocellulose as a natural source for groundbreaking applications in materials science: Today's state," *Materials Today*, vol. 21, no. 7, pp. 720–748, Sep. 2018, <https://doi.org/10.1016/j.mattod.2018.02.001>
- [6] D. Trache *et al.*, "Nanocellulose: From Fundamentals to Advanced Applications," *Frontiers in Chemistry*, vol. 8, May 2020, <https://doi.org/10.3389/fchem.2020.00392>
- [7] T. Puspaningrum, N. S. Indrasti, C. Indrawanto, and M. Yani, "Life cycle assessment of coconut plantation, copra, and charcoal production," *Global Journal of Environmental Science and Management*, vol. 9, no. 4, pp. 653–672, 2023, <https://doi.org/https://doi.org/10.22034/gjesm.2023.04.01>
- [8] Maryam and D. Rahmad, "Synthesis of nano bacterial cellulose using acid hydrolysis-ultrasonication treatment," *Journal of Physics: Conference Series*, vol. 1185, p. 012028, Apr. 2019, <https://doi.org/10.1088/1742-6596/1185/1/012028>
- [9] T. A. Nguyen and X. C. Nguyen, "Bacterial Cellulose-Based Biofilm Forming Agent Extracted from Vietnamese Nata-de-Coco Tree by Ultrasonic Vibration Method: Structure

- and Properties,” *Journal of Chemistry*, vol. 2022, pp. 1–10, Aug. 2022, <https://doi.org/10.1155/2022/7502796>
- [10] H. Abrial, V. Lawrensus, D. Handayani, and E. Sugiarti, “Preparation of nano-sized particles from bacterial cellulose using ultrasonication and their characterization,” *Carbohydrate Polymers*, vol. 191, pp. 161–167, Jul. 2018, <https://doi.org/10.1016/j.carbpol.2018.03.026>
- [11] N. Pandi, S. H. Sonawane, and K. Anand Kishore, “Synthesis of cellulose nanocrystals (CNCs) from cotton using ultrasound-assisted acid hydrolysis,” *Ultrasonics Sonochemistry*, vol. 70, p. 105353, Jan. 2021, <https://doi.org/10.1016/j.ultsonch.2020.105353>
- [12] R. A. A. Rusdi *et al.*, “Pre-treatment effect on the structure of bacterial cellulose from Nata de Coco (*Acetobacter xylinum*),” *Polimery*, vol. 67, no. 3, pp. 110–118, Mar. 2022, <https://doi.org/10.14314/polimery.2022.3.3>
- [13] R. Kose, I. Mitani, W. Kasai, and T. Kondo, “Nanocellulose” As a Single Nanofiber Prepared from Pellicle Secreted by *Gluconacetobacter xylinus* Using Aqueous Counter Collision,” *Biomacromolecules*, vol. 12, no. 3, pp. 716–720, Mar. 2011, <https://doi.org/10.1021/bm1013469>
- [14] J. Zhang, S. Xu, and W. Li, “High shear mixers: A review of typical applications and studies on power draw, flow pattern, energy dissipation and transfer properties,” *Chemical Engineering and Processing: Process Intensification*, vol. 57–58, pp. 25–41, Jul. 2012, <https://doi.org/10.1016/j.cep.2012.04.004>
- [15] A. Amri, Y. Bertilsya Hendri, C.-Y. Yin, M. Mahbubur Rahman, M. Altarawneh, and Z.-T. Jiang, “Very-few-layer graphene obtained from facile two-step shear exfoliation in aqueous solution,” *Chemical Engineering Science*, vol. 245, p. 116848, Dec. 2021, <https://doi.org/10.1016/j.ces.2021.116848>
- [16] E. L. Chan *et al.*, “Dem investigation of horizontal high shear mixer flow behaviour and implications for scale-up,” *Powder Technology*, vol. 270, pp. 561–568, Jan. 2015, <https://doi.org/10.1016/j.powtec.2014.09.017>
- [17] H. Zhang, C. Chen, C. Zhu, and D. Sun, “Production of bacterial cellulose by acetobacter xylinum: Effects of carbon/nitrogen-ratio on cell growth and metabolite production,” *Cellulose Chemistry and Technology*, vol. 50, no. 9, pp. 997–1003, 2016, [Online]. Available: [https://www.cellulosechemtechnol.ro/pdf/CCT9-10\(2016\)/p.997-1003.pdf](https://www.cellulosechemtechnol.ro/pdf/CCT9-10(2016)/p.997-1003.pdf)
- [18] M. E. C. C. Carvalho *et al.*, “Low back pain during pregnancy,” *Brazilian Journal of Anesthesiology (English Edition)*, vol. 67, no. 3, pp. 266–270, May 2017, <https://doi.org/10.1016/j.bjane.2015.08.014>
- [19] O. Regina, H. Sudrajad, and D. Syaflita, “Measurement of viscosity uses an alternative viscometer,” *Jurnal Geliqa Sains: Jurnal Pendidikan Fisika*, vol. 6, no. 2, p. 127, Feb. 2019, <https://doi.org/10.31258/jgs.6.2.127-132>
- [20] S. Fatimah, R. Ragadhita, D. F. Al Husaeni, and A. B. D. Nandiyanto, “How to Calculate Crystallite Size from X-Ray Diffraction (XRD) using Scherrer Method,” *ASEAN Journal of Science and Engineering*, vol. 2, no. 1, pp. 65–76, Jun. 2021, <https://doi.org/10.17509/ajse.v2i1.37647>
- [21] S. Nam, A. D. French, B. D. Condon, and M. Concha, “Segal crystallinity index revisited by the simulation of X-ray diffraction patterns of cotton cellulose I β and cellulose II,” *Carbohydrate Polymers*, vol. 135, pp. 1–9, Jan. 2016, <https://doi.org/10.1016/j.carbpol.2015.08.035>
- [22] O. Nechyporchuk, F. Pignon, and M. N. Belgacem, “Morphological properties of nanofibrillated cellulose produced using wet grinding as an ultimate fibrillation process,” *Journal of Materials Science*, vol. 50, no. 2, pp. 531–541, Jan. 2015, <https://doi.org/10.1007/s10853-014-8609-1>
- [23] X. T. Zheng, H. J. Wang, Y. Liu, D. M. Wu, Z. L. Zhao, and X. X. He, “Influence of Light Scattering Particles on Optical Properties of Polymer Diffusion Plate,” *Key Engineering*

- Materials*, vol. 562–565, pp. 984–990, Jul. 2013, <https://doi.org/10.4028/www.scientific.net/KEM.562-565.984>
- [24] L. Liu, Z. Shen, M. Yi, X. Zhang, and S. Ma, “A green, rapid and size-controlled production of high-quality graphene sheets by hydrodynamic forces,” *RSC Advances*, vol. 4, no. 69, pp. 36464–36470, 2014, <https://doi.org/10.1039/C4RA05635C>
- [25] W. Wu, N. G. Tassi, H. Zhu, Z. Fang, and L. Hu, “Nanocellulose-based Translucent Diffuser for Optoelectronic Device Applications with Dramatic Improvement of Light Coupling,” *ACS Applied Materials & Interfaces*, vol. 7, no. 48, pp. 26860–26864, Dec. 2015, <https://doi.org/10.1021/acsami.5b09249>
- [26] R. Suliman, “Evaluation of the Absorbance and Transmittance of the Optical Light for Three Different Types of Composite Resin Stored in Artificial Saliva (in vitro study),” *Al-Rafidain Dental Journal*, vol. 17, no. 1, pp. 86–97, Nov. 2016, <https://doi.org/10.33899/rden.2016.164142>
- [27] X. F. Xu, P. J. Bates, and G. Zak, “Effect of glass fiber and crystallinity on light transmission during laser transmission welding of thermoplastics,” *Optics & Laser Technology*, vol. 69, pp. 133–139, Jun. 2015, <https://doi.org/10.1016/j.optlastec.2014.12.025>
- [28] A. H. Yuwono *et al.*, “Controlling the crystallinity and nonlinear optical properties of transparent TiO₂–PMMA nanohybrids,” *Journal of Materials Chemistry*, vol. 14, no. 20, pp. 2978–2987, 2004, <https://doi.org/10.1039/B403530E>
- [29] Z. Fan, J. Chen, S. Sun, and Q. Zhou, “A novel strategy to reduce the viscosity of cellulose-ionic liquid solution assisted by transition metal ions,” *Carbohydrate Polymers*, vol. 256, p. 117535, Mar. 2021, <https://doi.org/10.1016/j.carbpol.2020.117535>
- [30] T. Lindström, “Aspects on nanofibrillated cellulose (NFC) processing, rheology and NFC-film properties,” *Current Opinion in Colloid & Interface Science*, vol. 29, pp. 68–75, May 2017, <https://doi.org/10.1016/j.cocis.2017.02.005>
- [31] M. A. Hubbe *et al.*, “Rheology of nanocellulose-rich aqueous suspensions: A Review,” *Bioresources*, vol. 12, no. 4, pp. 9556–9661, 2017, <https://doi.org/10.15376/biores.12.4.Hubbe>
- [32] R. A. Ahmad Rusdi, Z. H. Z. Abidin, H. A. Tajuddin, F. Abdul Aziz, and N. Abdul Halim, “Comparative Study of Chemical and Mechanical Treatment Effects on Bacterial Cellulose from Nata de Coco,” *Materials Science Forum*, vol. 888, pp. 256–261, Mar. 2017, <https://doi.org/10.4028/www.scientific.net/MSF.888.256>
- [33] N. Siddiqui, R. H. Mills, D. J. Gardner, and D. Bousfield, “Production and Characterization of Cellulose Nanofibers from Wood Pulp,” *Journal of Adhesion Science and Technology*, vol. 25, no. 6–7, pp. 709–721, Jan. 2011, <https://doi.org/10.1163/016942410X525975>
- [34] Z. Li *et al.*, “Robust All-Cellulose Nanofiber Composite from Stack-Up Bacterial Cellulose Hydrogels via Self-Aggregation Forces,” *Journal of Agricultural and Food Chemistry*, vol. 68, no. 9, pp. 2696–2701, Mar. 2020, <https://doi.org/10.1021/acs.jafc.9b07671>
- [35] A. Solikhin, Y. S. Hadi, M. Y. Massijaya, and S. Nikmatin, “Morphological, Chemical, and Thermal Characteristics of Nanofibrillated Cellulose Isolated Using Chemo-mechanical Methods,” *Makara Journal of Science*, vol. 21, no. 2, Jul. 2017, <https://doi.org/10.7454/mss.v21i2.6085>
- [36] S. W. Gadzama, O. K. Sunmonu, U. S. Isiaku, and A. Danladi, “Isolation and characterization of nanocellulose from pineapple leaf fibres via chemo-mechanical method,” *Science World Journal*, vol. 15, no. 2, 2020, Accessed: Dec. 29, 2024. [Online]. Available: <https://www.ajol.info/index.php/swj/article/view/202955>
- [37] R. Aryasena, Kusmono, and N. Umami, “Production of cellulose nanocrystals extracted from Pennisetum purpureum fibers and its application as a lubricating additive in engine oil,” *Heliyon*, vol. 8, no. 11, p. e11315, Nov. 2022, <https://doi.org/10.1016/j.heliyon.2022.e11315>
- [38] N. Halib, M. C. I. M. Amin, and I. Ahmad, “Physicochemical Properties and Characterization of Nata de Coco from Local Food Industries as a Source of Cellulose,” *Sains*

- Malays, vol. 41, no. 2, 2012, [Online]. Available: http://www.ukm.edu.my/jsm/pdf_files/SM-PDF-41-2-2012/08%20Nadia.pdf
- [39] S. Y. Oh *et al.*, “Crystalline structure analysis of cellulose treated with sodium hydroxide and carbon dioxide by means of X-ray diffraction and FTIR spectroscopy,” *Carbohydrate Research*, vol. 340, no. 15, pp. 2376–2391, Oct. 2005, <https://doi.org/10.1016/j.carres.2005.08.007>
- [40] D. Zhao *et al.*, “Exploring structural variations of hydrogen-bonding patterns in cellulose during mechanical pulp refining of tobacco stems,” *Carbohydrate Polymers*, vol. 204, pp. 247–254, Jan. 2019, <https://doi.org/10.1016/j.carbpol.2018.10.024>
- [41] M. K. Bin Bakri and E. Jayamani, “Comparative study of functional groups in natural fibers: Fourier Transform Infrared Analysis (FTIR),” in *International Conference on Futuristic Trends in Engineering, Science, Humanities, and Technology (FTESHT-16)*, P. S. Chauhan, Ed., Gwalior: IPS Group of Colleges, Jan. 2016, pp. 167–174. [Online]. Available: <https://www.troindia.in/proceeding/vol-1%20proceeding.pdf>
- [42] A. C. W. Leung *et al.*, “Characteristics and Properties of Carboxylated Cellulose Nanocrystals Prepared from a Novel One-Step Procedure,” *Small*, vol. 7, no. 3, pp. 302–305, Feb. 2011, <https://doi.org/10.1002/sml.201001715>
- [43] N. Kruer-Zerhusen, B. Cantero-Tubilla, and D. B. Wilson, “Characterization of cellulose crystallinity after enzymatic treatment using Fourier transform infrared spectroscopy (FTIR),” *Cellulose*, vol. 25, no. 1, pp. 37–48, Jan. 2018, <https://doi.org/10.1007/s10570-017-1542-0>
- [44] B. Deepa *et al.*, “Utilization of various lignocellulosic biomass for the production of nanocellulose: a comparative study,” *Cellulose*, vol. 22, no. 2, pp. 1075–1090, Apr. 2015, <https://doi.org/10.1007/s10570-015-0554-x>
- [45] Y. Wang, Y. He, J. Zhan, and Z. Li, “Identification of soil particle size distribution in different sedimentary environments at river basin scale by fractal dimension,” *Scientific Reports*, vol. 12, no. 1, p. 10960, Jun. 2022, <https://doi.org/10.1038/s41598-022-15141-6>
- [46] C. J. U. Espinoza, F. Alberini, O. Mihailova, A. J. Kowalski, and M. J. H. Simmons, “Flow, turbulence and potential droplet break up mechanisms in an in-line Silverson 150/250 high shear mixer,” *Chemical Engineering Science: X*, vol. 6, p. 100055, Feb. 2020, <https://doi.org/10.1016/j.cesx.2020.100055>
- [47] M. Pääkkö *et al.*, “Enzymatic Hydrolysis Combined with Mechanical Shearing and High-Pressure Homogenization for Nanoscale Cellulose Fibrils and Strong Gels,” *Biomacromolecules*, vol. 8, no. 6, pp. 1934–1941, Jun. 2007, <https://doi.org/10.1021/bm061215p>
- [48] V. Burlakov and A. Goriely, “Thermodynamic limit for particle monodispersity: How narrow can a particle size distribution be?,” *EPL (Europhysics Letters)*, vol. 119, no. 5, p. 50001, Sep. 2017, <https://doi.org/10.1209/0295-5075/119/50001>
- [49] A. Bertran, S. Sandoval, J. Oró-Solé, À. Sánchez, and G. Tobias, “Particle size determination from magnetization curves in reduced graphene oxide decorated with monodispersed superparamagnetic iron oxide nanoparticles,” *Journal of Colloid and Interface Science*, vol. 566, pp. 107–119, Apr. 2020, <https://doi.org/10.1016/j.jcis.2020.01.072>
- [50] R. A. Araujo, A. F. Rubira, H. D. M. Follmann, and R. Silva, “Fast and facile size selection processing for high quality cellulose nanowhiskers,” *Cellulose*, vol. 27, no. 1, pp. 205–214, Jan. 2020, <https://doi.org/10.1007/s10570-019-02790-6>
- [51] Y. Li and C.-W. Park, “Particle Size Distribution in the Synthesis of Nanoparticles Using Microemulsions,” *Langmuir*, vol. 15, no. 4, pp. 952–956, Feb. 1999, <https://doi.org/10.1021/la980550z>
- [52] M. F. Rosa *et al.*, “Cellulose nanowhiskers from coconut husk fibers: Effect of preparation conditions on their thermal and morphological behavior,” *Carbohydrate Polymers*, vol. 81, no. 1, pp. 83–92, May 2010, <https://doi.org/10.1016/j.carbpol.2010.01.059>

- [53] J. D. Hernandez-Varela, J. J. Chanona-Perez, S. L. Villasenor-Altamirano, C. Mendoza-Martinez, and F. Cervantes Sodi, “Changes of crystallinity index and crystallite size in cotton cellulose nanopar by ball milling,” in *2020 17th International Conference on Electrical Engineering, Computing Science and Automatic Control (CCE)*, IEEE, Nov. 2020, pp. 1–6. <https://doi.org/10.1109/CCE50788.2020.9299162>
- [54] S.-C. Shi, C.-F. Hsieh, and D. Rahmadiawan, “Enhancing mechanical properties of polylactic acid through the incorporation of cellulose nanocrystals for engineering plastic applications,” *Teknomekanik*, vol. 7, no. 1, pp. 20–28, May 2024, <https://doi.org/10.24036/teknomekanik.v7i1.30072>
- [55] M. Nogi, C. Kim, T. Sugahara, T. Inui, T. Takahashi, and K. Sukanuma, “High thermal stability of optical transparency in cellulose nanofiber paper,” *Applied Physics Letters*, vol. 102, no. 18, May 2013, <https://doi.org/10.1063/1.4804361>